

A-3-3 Aquifer Sr-90 Simulation Results

Predicted Sr-90 concentrations in the aquifer through year 2096 on the coarse grid are shown in Figure A-3-9 and through the year 2151 on the fine grid in Figure A-3-10. These can be compared to the RI/BRA base case results shown in Figures J-8-18 and J-8-19 (RI/BRA) [DOE-NE-ID 2006]. Resultant peak aquifer concentrations for both simulations are shown in Figure A-3-11, with this simulation shown in red and the RI/BRA base case shown in black. These figures illustrate three important performance measures. The first performance measure is the peak concentration in year 2095, the second is the time during which the MCL is exceeded, and the third is the areal extent contaminated above the MCL.

In 2095, removing the relatively large volume of water from the middle reach of the Big Lost River has reduced the peak concentration from 18.6 pCi/L to 17.5 pCi/L, a difference of only 6%. As shown by the vertical concentration plots in Figure A-3-6, high concentrations are predicted to exist north of the tank farm at shallow depths. However, at depths approaching the vadose zone-aquifer interface, the higher concentrations exist further south. As shown in Figure A-3-3, the southern extent of the Big Lost River is confined to the north at shallow depths and just reaches the tank farm at the 100- to 140-m depth interval. This simulation suggests that the high recharge rates from Big Lost River infiltration do not overlap with the high concentrations nearer the tank farm. This distribution is reflected in Figure A-3-11 where, during the time period prior to year 2095, the peak concentration in this simulation is very similar to that obtained in the RI/BRA base case. The effect of removing the Big Lost River fluxes occurs at about the same time the anthropogenic water is removed in year 2095.

Although the 2095 peak concentration in this case was not greatly reduced, removing this large water volume allows concentrations to fall below the MCL by year 2121. This second performance measure suggests that by removing influx from the middle reach of the Big Lost River, the MCL can be achieved only 8 years earlier than if this water is not removed.

Figure A-3-9 and Figure J-8-18 [DOE-NE-ID 2006] show that removing infiltration along the middle reach of the Big Lost River has a relatively small affect on the areal extent of contamination above the MCL prior to year 2096. The fine-scale contours shown in Figures A-3-10 and Figure J-8-19 [DOE-NE-ID 2006] show that removing the Big Lost River fluxes mainly affects concentrations below 0.8 pCi/L (black contour lines) in the region north of the tank farm where the predicted concentrations were originally below 8 pCi/L in the RI/BRA base model. These fine-scale contours reflect the removal of flux in that region as the 0.8 pCi/L contour recedes to the area south of the tank farm, leaving a very small isolated region to the northeast through year 2095. In the sensitivity simulations presented in Appendix J of the RI/BRA [DOE-NE-ID 2006], this isolated region to the north was a continued hot spot in many of the simulations where the interbed K_d was lower. With the increased interbed K_d , Sr-90 does not move as far north from the tank farm, and, in this simulation, the Sr-90 that does is essentially immobile in the upper interbeds. By year 2151, the area contaminated above the 0.8 pCi/L level is significantly reduced and is confined to an area north of the former percolation ponds and south of the tank farm.

Removing the Big Lost River fluxes allows the Sr-90 above the MCL to remain essentially south of the tank farm and north of the former percolation ponds after year 2040. In comparison to the RI/BRA results, removing this relatively large volumetric infiltration in northern INTEC has a relatively small impact on the overall distribution of Sr-90 contamination above the MCL.

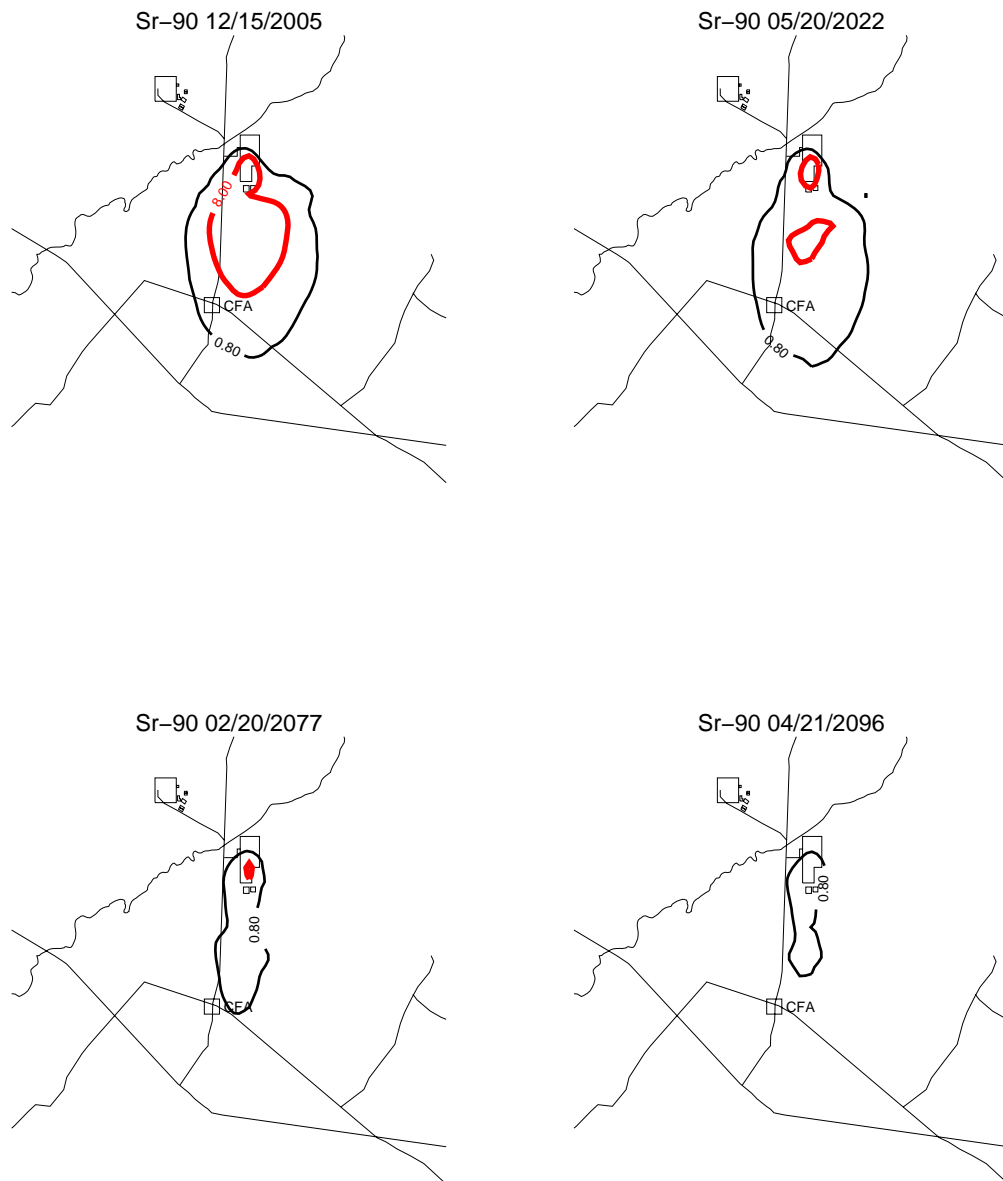


Figure A-3-9. Aquifer concentrations (horizontal contours) after preventing infiltration from the Big Lost River (pCi/L) (MCL = thick red line, 10*MCL=thin red line, MCL/10 = black line).



Figure A-3-10. Aquifer concentrations (horizontal contours) after preventing infiltration from the Big Lost River (pCi/L) (continued) (MCL = thick red line, 10*MCL=thin red line, MCL/10 = black line).

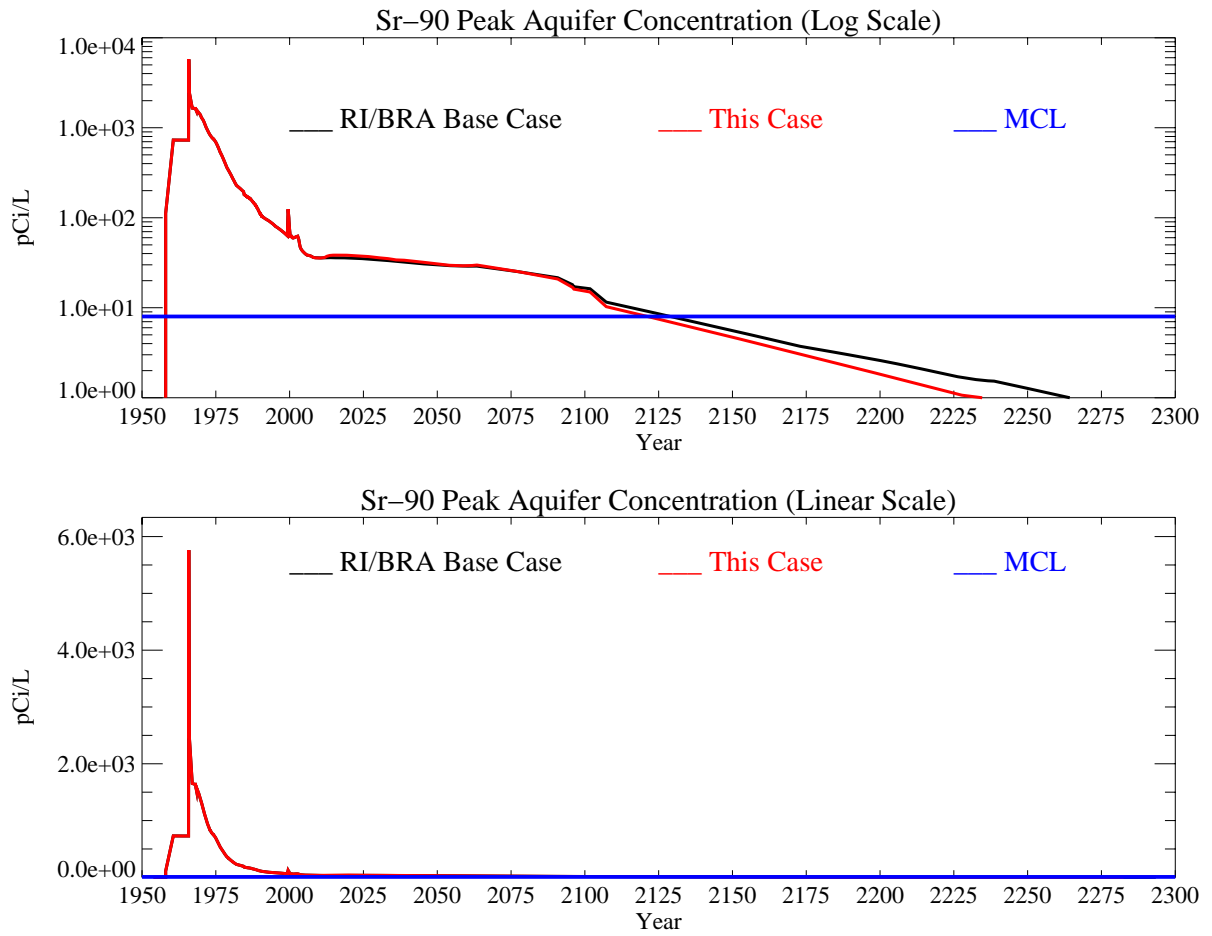


Figure A-3-11. Peak aquifer concentrations (pCi/L) preventing infiltration from the Big Lost River (MCL = blue line, model predicted = black line [base case] and red line [this case]).

A-4 IMMOBILIZING Sr-90 IN THE TANK FARM ALLUVIUM

The purpose of this simulation is to determine the effect of immobilizing Sr-90 remaining in the alluvium in year 2008. This simulation mimics the effects of either source removal or in situ stabilization. It is implemented in the model by changing the alluvium Sr-90 K_d in the area of the four 100- X 100-m horizontal grid blocks in the base vadose zone model that spans the 10 acres surrounding the tank farm represented by the shaded area in Figure A-4-1. In this area, the K_d was increased from 2 mL/g to 100,000 mL/g in the year 2008. This increase effectively prevents Sr-90 from migrating from the alluvium but does not alter the infiltration rate through this 200- X 200-m region. As a result, 18 cm/yr precipitation infiltration and 4 cm/yr infiltration from anthropogenic water continue to play an advective and dispersive role in transport through the alluvium and from the underlying perched water. Sources of Sr-90 placed in the base model grid affected by this change include the residual from CPP-31 (3,564 Ci), CPP-36/91 (53.8 Ci), and CPP-41 (7.17 E-3 Ci). Because the 3,564 Ci remaining after 20 years following the CPP-31 release is much larger than the other two OU 3-13 soil sites, this simulation is equivalent to immobilizing Sr-90 remaining at Site CPP-31. All other sources outside of this area were placed in the submodel grid and are transported through the alluvium with a K_d of 20 mL/g.

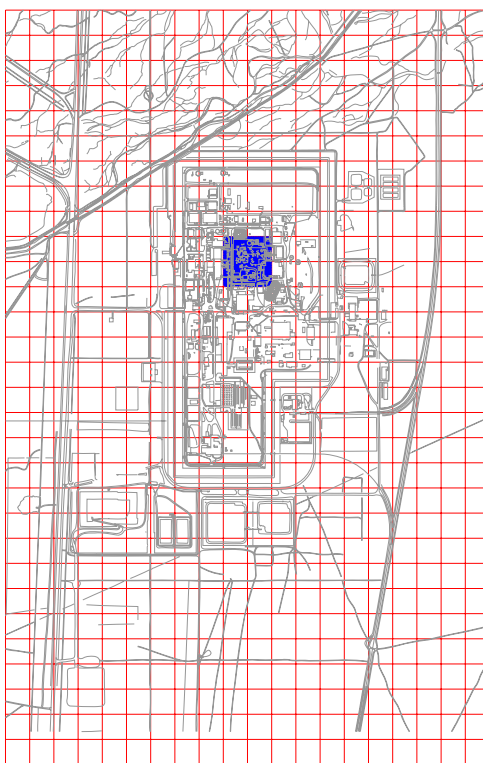


Figure A-4-1. Area in which Sr-90 is immobilized in the tank farm alluvium.

A-4-1 Vadose Zone Sr-90 Simulation Results

The predicted distribution of Sr-90 in the vadose zone is shown in Figures A-4-2 and A-4-3 through the year 2293 and can be compared to Figures J-8-10 through J-8-13 [DOE-NE-ID 2006]. Peak vadose zone concentrations through time for this simulation are shown in red on Figure A-4-4 and are equivalent to the RI/BRA base case (black) prior to year 2008 when the K_d for Sr-90 in the tank farm alluvium was raised to 100,000 mL/g to simulate immobilization. The partition coefficient is essentially the ratio of aqueous-phase Sr-90 to sorbed-phase Sr-90. Increasing the K_d re-partitions the aqueous-phase Sr-90 onto the solids and results in a decrease in aqueous concentration. The differences in peak vadose zone concentrations following this increase in K_d show that the highest concentrations are alluvium pore water concentrations, as opposed to being concentrations in the lower interbeds.

The rate at which the activity enters the aquifer from the vadose zone is given in Figure A-4-5. Immobilizing the Sr-90 remaining in the tank farm alluvium has essentially no effect on the migration of Sr-90 from the vadose zone into the aquifer. In this simulation and in the RI/BRA base case 3,564 Ci (undecayed) were predicted to remain in the alluvium 20 years after the CPP-31 release. The negligible difference between mobilizing Sr-90 in the tank farm alluvium at a K_d of 2 mL/g and immobilization via a very high K_d suggests that the Sr-90 remaining in the alluvium does not contribute significantly to aquifer concentrations.

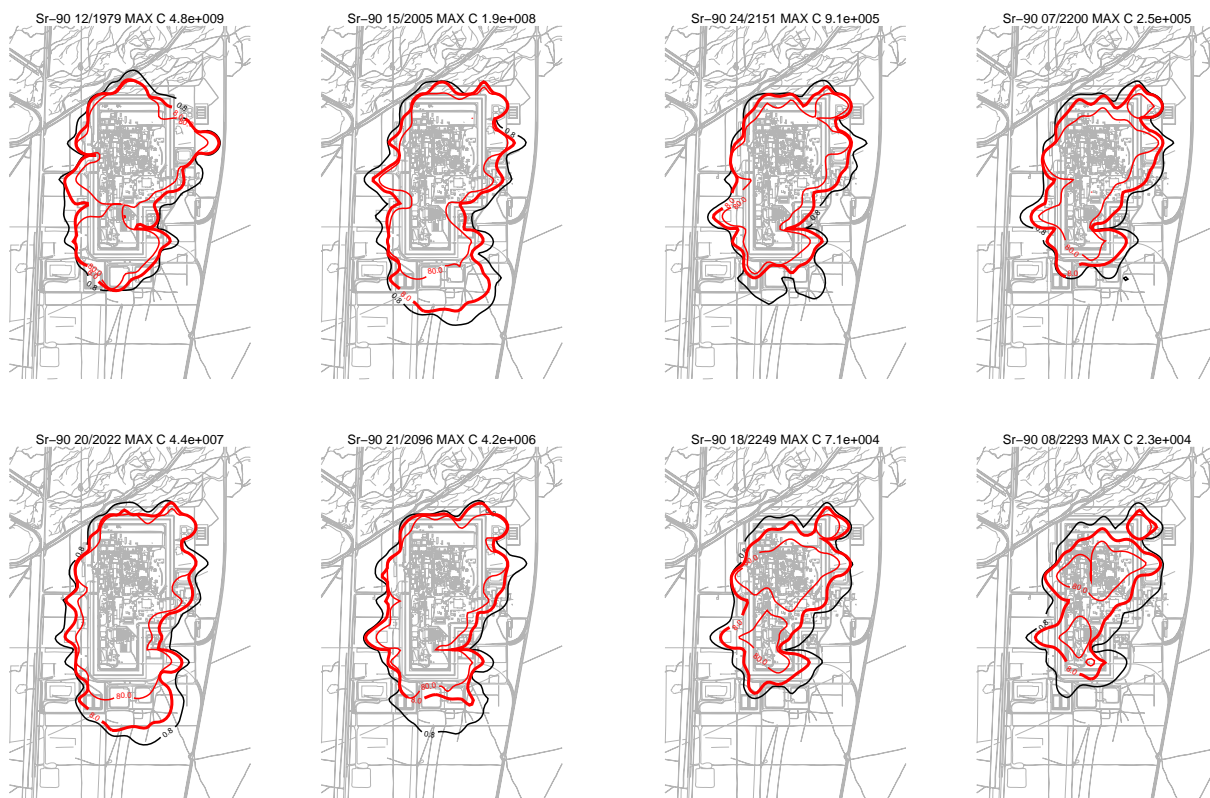


Figure A-4-2. Vadose zone concentrations (horizontal contours) (pCi/L) immobilizing Sr-90 in the tank farm alluvium (MCL = thick red line, 10*MCL=thin red line, MCL/10 = black line).

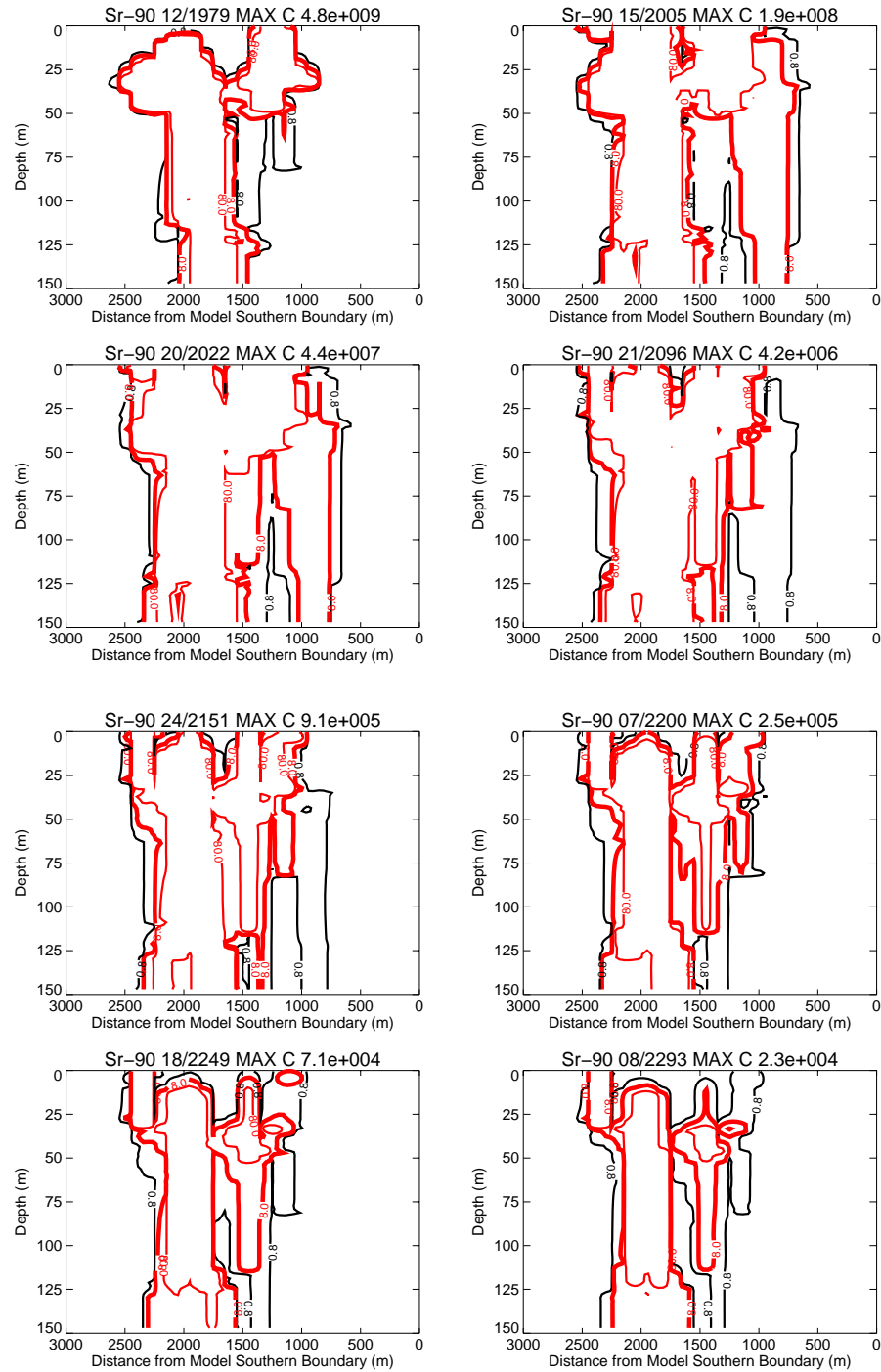


Figure A-4-3. Vadose zone concentrations (vertical contours) (pCi/L) immobilizing Sr-90 in the tank farm alluvium (MCL = thick red line, 10*MCL=thin red line, MCL/10 = black line).

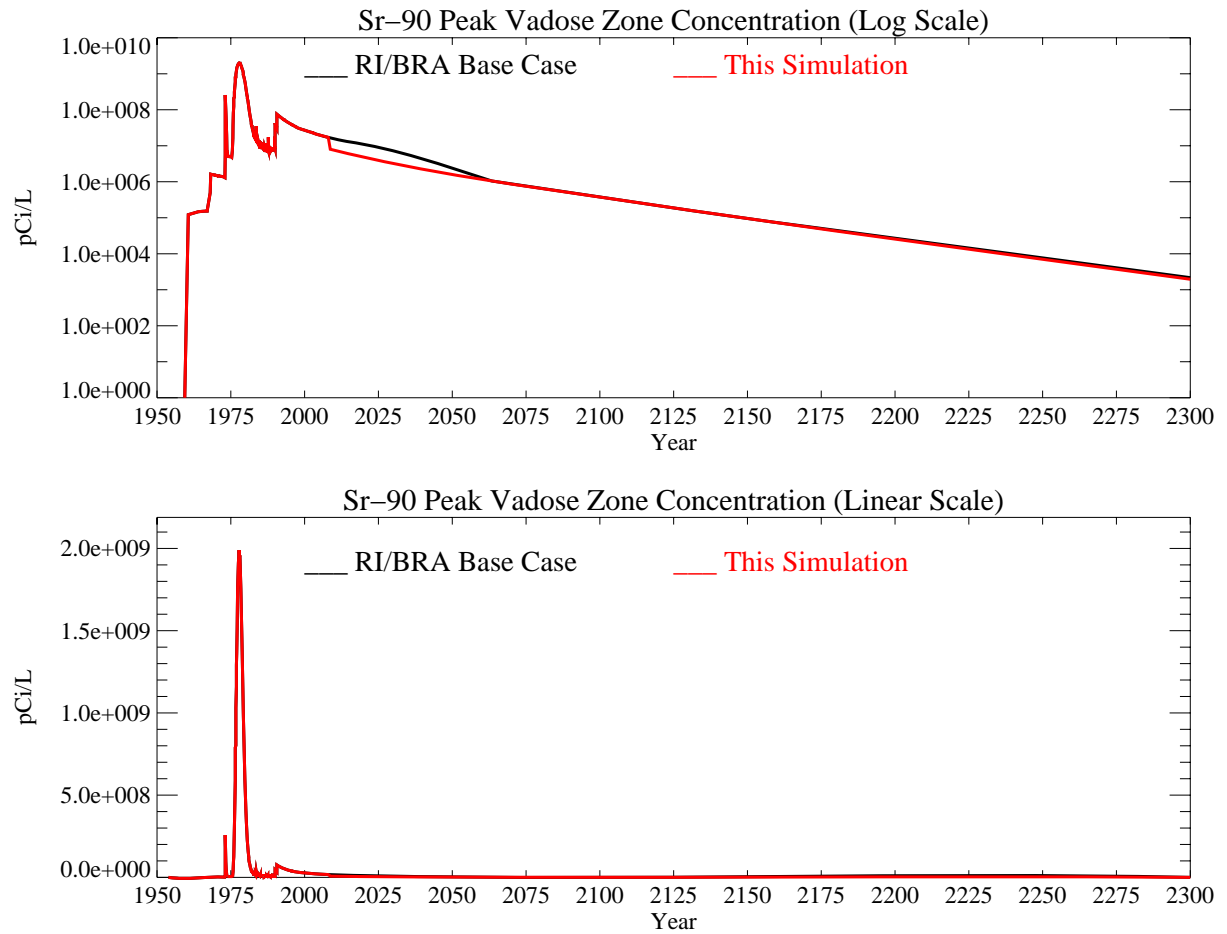


Figure A-4-4. Peak vadose zone concentrations (pCi/L) immobilizing Sr-90 in the tank farm alluvium (MCL = blue line, model predicted = black line [base case] and red line [this case]).

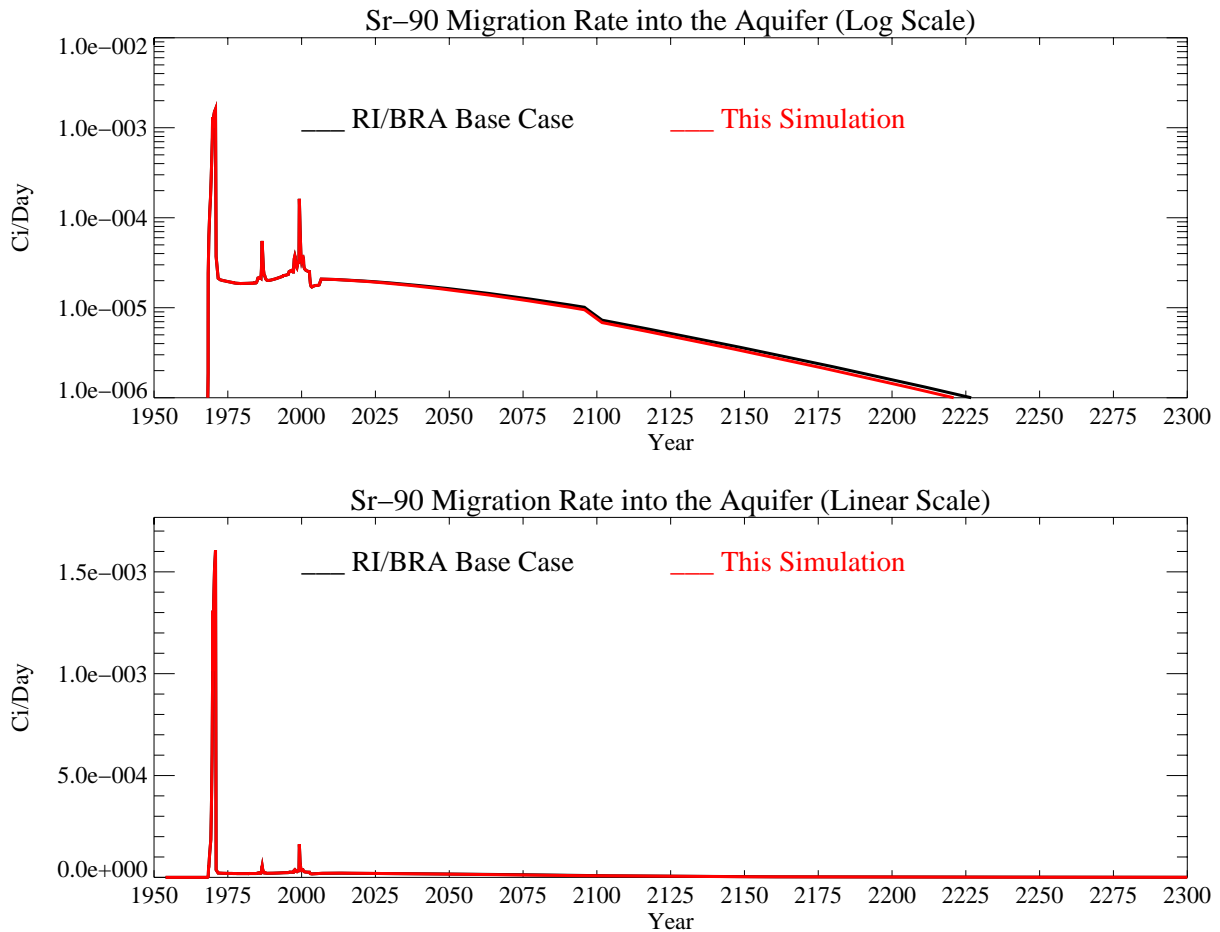


Figure A-4-5. Activity flux into the aquifer immobilizing Sr-90 in the tank farm alluvium (Ci/day).

A-4-2 Aquifer Sr-90 Simulation Results

Predicted Sr-90 concentrations in the aquifer through year 2096 on the course grid are shown in Figure A-4-6 and through the year 2151 on the fine grid in Figure A-4-7. These can be compared to the RI/BRA base case results shown in Figures J-8-18 and J-8-19 [DOE-NE-ID 2006]. Resultant peak aquifer concentrations for both simulations are shown in Figure A-4-8, with this simulation shown in red, and the RI/BRA base case shown in black. Based on the three performance measures of peak concentration in year 2095, the time during which the MCL is exceeded, and the areal extent contaminated above the MCL, immobilizing Sr-90 remaining in the alluvium will be marginally beneficial.

In 2095, the predicted peak concentration is 16.9 pCi/L which is slightly less than the value obtained in the RI/BRA base case (18.6 pCi/L). Concentrations are predicted to exceed the MCL through year 2122, which is 7 years earlier than predicted in the RI/BRA base case. The third performance measure is the area impacted above the MCL, and comparison of Figure A-4-7 to Figure J-8-19 [DOE-NE-ID 2006] shows that there is essentially no change relative to the RI/BRA base case as a result of immobilizing Sr-90 in the tank farm alluvium. This indicates that, in the RI/BRA base model, the Sr-90 remaining in the alluvium does not contribute significantly to aquifer contamination and that immobilizing Sr-90 in the alluvium will not result in lowering aquifer concentrations below the MCL by year 2095.

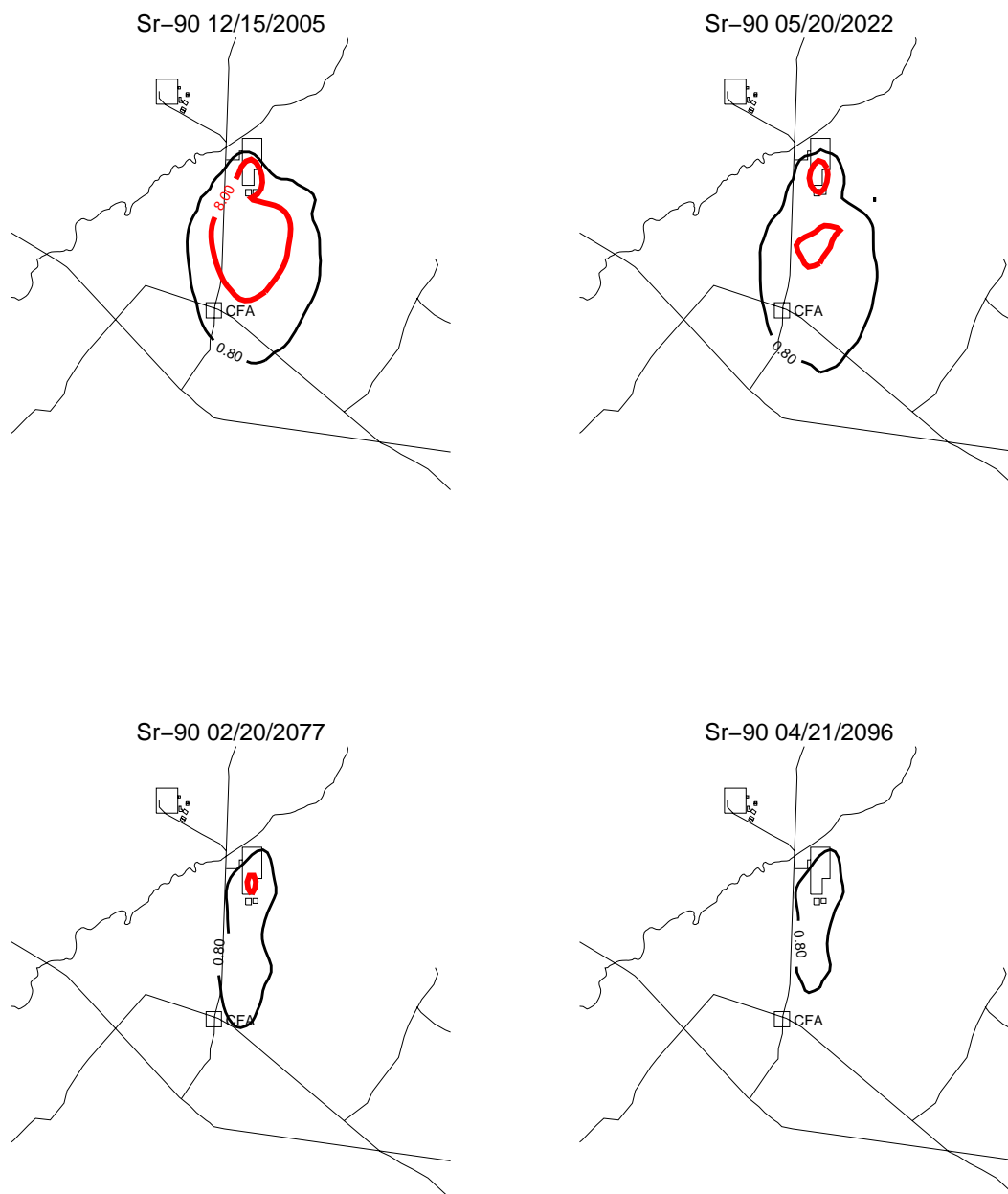


Figure A-4-6. Aquifer concentrations (horizontal contours) immobilizing Sr-90 in the alluvium (pCi/L) (MCL = thick red line, 10*MCL=thin red line, MCL/10 = black line).



Figure A-4-7. Aquifer concentrations (horizontal contours) (pCi/L) immobilizing Sr-90 in the alluvium (continued) (MCL = thick red line, 10*MCL=thin red line, MCL/10 = black line).

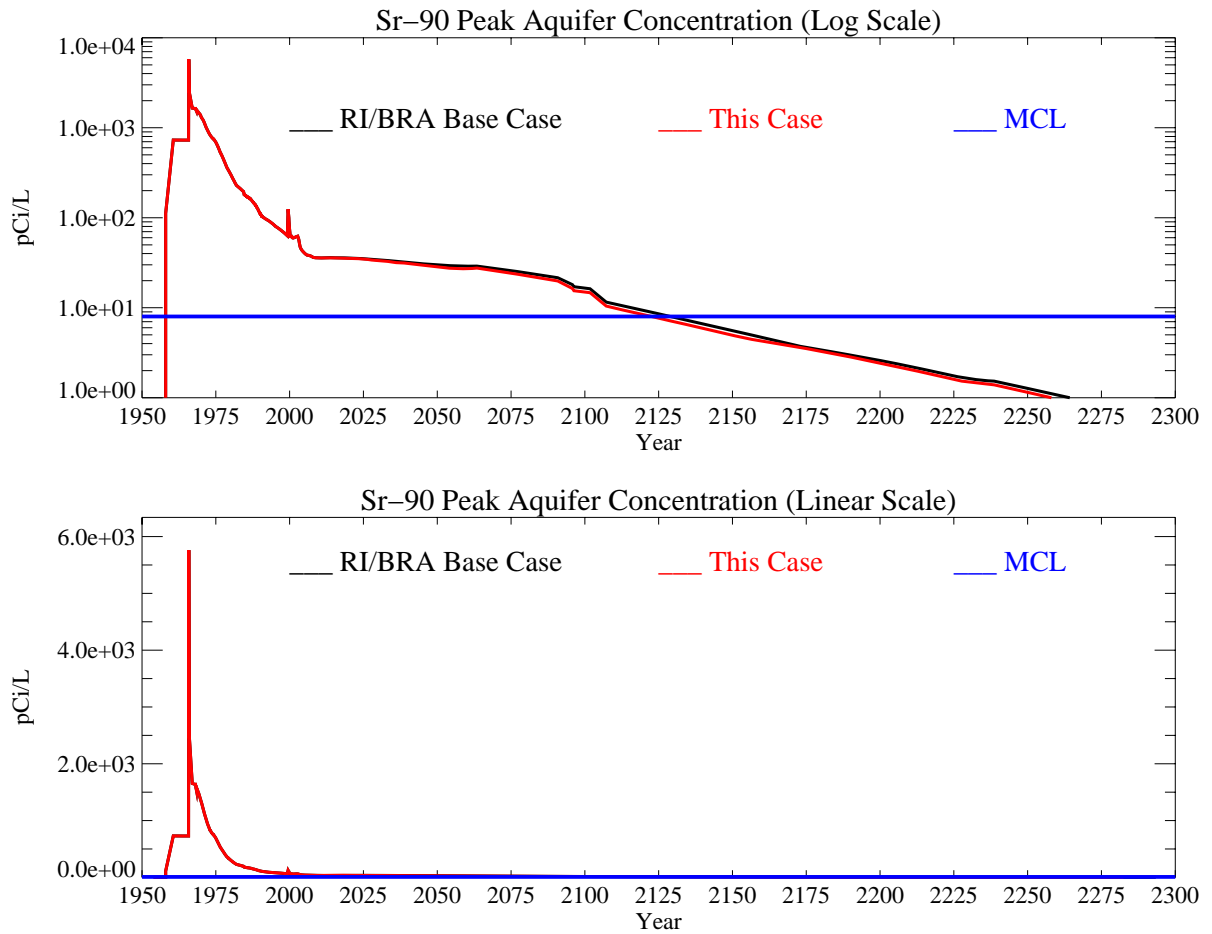


Figure A-4-8. Peak aquifer concentrations after immobilizing Sr-90 in the tank farm (pCi/L) with the MCL in blue, RI/BRA model in black, and this simulation in red.

A-5 REDUCING INFILTRATION THROUGH THE 10-ACRES SURROUNDING THE TANK FARM

The purpose of this simulation is to determine the effect of reducing infiltration in an area surrounding the tank farm relative to the RI/BRA base case. Roughly 4 cm/yr from anthropogenic water and 18 cm/yr from precipitation infiltrate through the area represented by the shaded area in Figure A-5-1 in the RI/BRA base model. By eliminating the anthropogenic water losses and/or greatly reducing precipitation infiltration through the tank farm, Sr-90 movement out of the tank farm alluvium will be reduced to diffusion only. The remedial design for a capillary or other type of infiltration-reducing barrier is not assessed here, but the hypothetical effects are examined by including a total infiltration of 0.1 cm/yr in the 40,000-m² (10-acre) area represented by the shaded area in Figure A-5-1. By reducing precipitation infiltration in the area surrounding the tank farm, recharge through the underlying perched water will be affected. In this simulation, we assume that the reductions in infiltration occur in year 2012 and that they are instantly effective.

Reducing infiltration through this relatively large area will result in (a) decreased dilution as the fresh-water recharge is removed; (b) slower migration from the vadose zone while en route to the aquifer for high concentration contaminants affected by this recharge; (c) increased residence time for Sr-90 in the vadose zone, allowing for more decay to occur en route to the aquifer; and (d) reduced lateral and longitudinal dispersion along the flow path, potentially increasing vadose zone concentrations while reducing the areal extent. These competing effects will primarily affect transport of contaminants in southern INTEC.

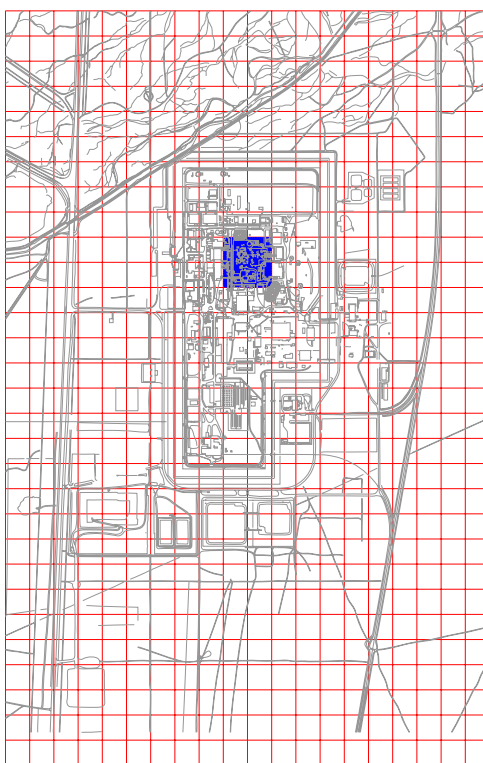


Figure A-5-1. Vadose zone simulation area showing the area affected by infiltration reduction.

A-5-1 Vadose Zone Sr-90 Simulation Results

The distribution of Sr-90 in the vadose zone is shown in Figures A-5-2 and A-5-3 through the year 2293 and can be compared to the base case shown in Figures J-8-10 through J-8-13 [DOE-NE-ID 2006]. The peak vadose zone concentrations through time are given in Figure A-5-4. The spatial distribution of Sr-90 in the vadose zone between the 0.8 pCi/L and 80 pCi/L levels is not significantly changed by reducing infiltration through the 10 acres surrounding the tank farm. This implies that monitoring the effectiveness of this remedy will require monitoring in areas of peak concentrations.

The peak vadose zone concentrations after removing the tank farm infiltration are higher than obtained in the base case during the 2015-2160 time period. This is a result of removing fresh-water recharge from infiltration causing higher concentrations of Sr-90 in the vadose zone pore water. Without considering the effect of this dilution, higher resultant concentrations in the perched water might be construed as increased arrival from the vadose zone. However, these higher pore water concentrations are offset by lower infiltration velocities, and, therefore, there is not an increase in migration rate into the aquifer (Figure A-5-5).

As shown in Figure A-5-5, there is a significant decrease in predicted flux rates out of the vadose zone following the reduction in fluxes through the tank farm. As shown by the red line representing this simulation and compared to the RI/BRA base case (shown in black), reducing fluxes through the tank farm results in an almost immediate decrease in Sr-90 entering the aquifer. Integrated through time, there is a total of 1.53 Ci of Sr-90 entering the aquifer from the vadose zone. This is roughly equal to the total of 1.52 Ci entering the aquifer following the removal of Big Lost River flux: The difference between these two scenarios is in the area affected. In this case, the fluxes are reduced in central INTEC, and, in the former, the fluxes were reduced in northern INTEC.

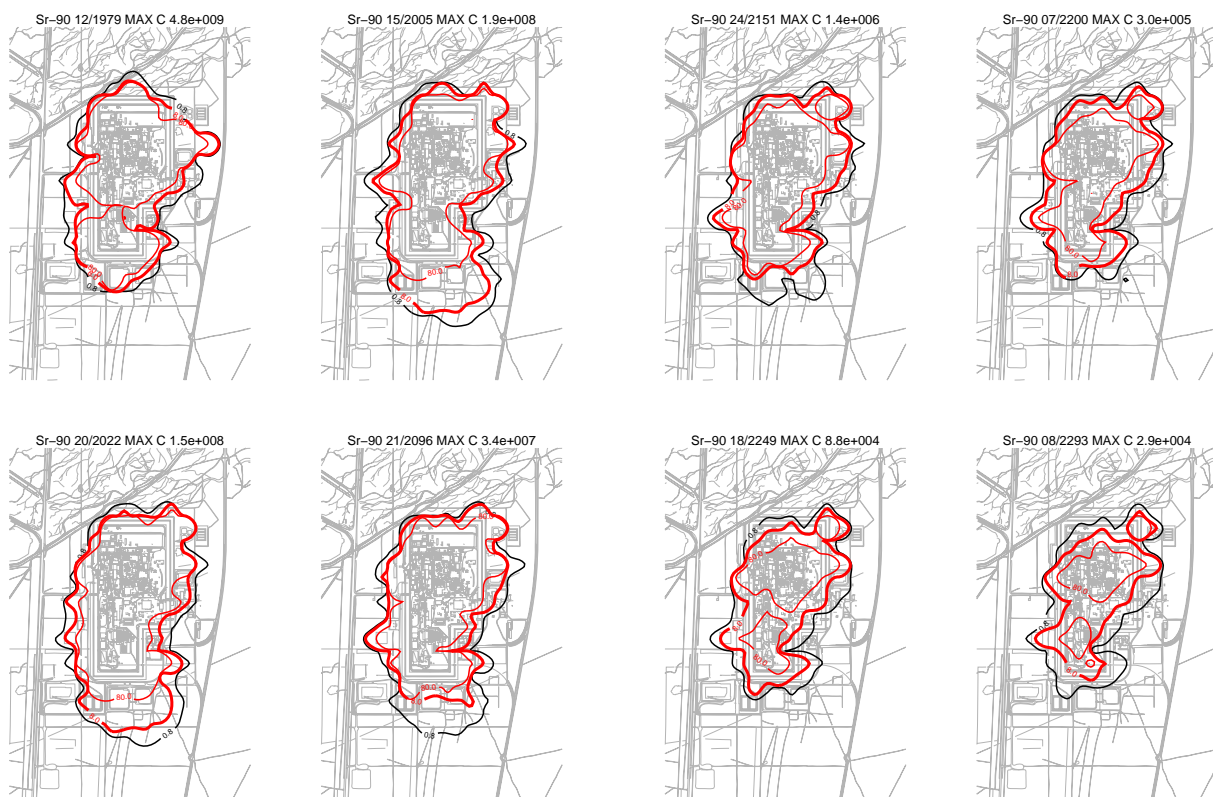


Figure A-5-2. Vadose zone concentrations (horizontal contours) (pCi/L) reducing infiltration through the area surrounding the tank farm (MCL = thick red line, 10*MCL=thin red line, MCL/10 = black line).

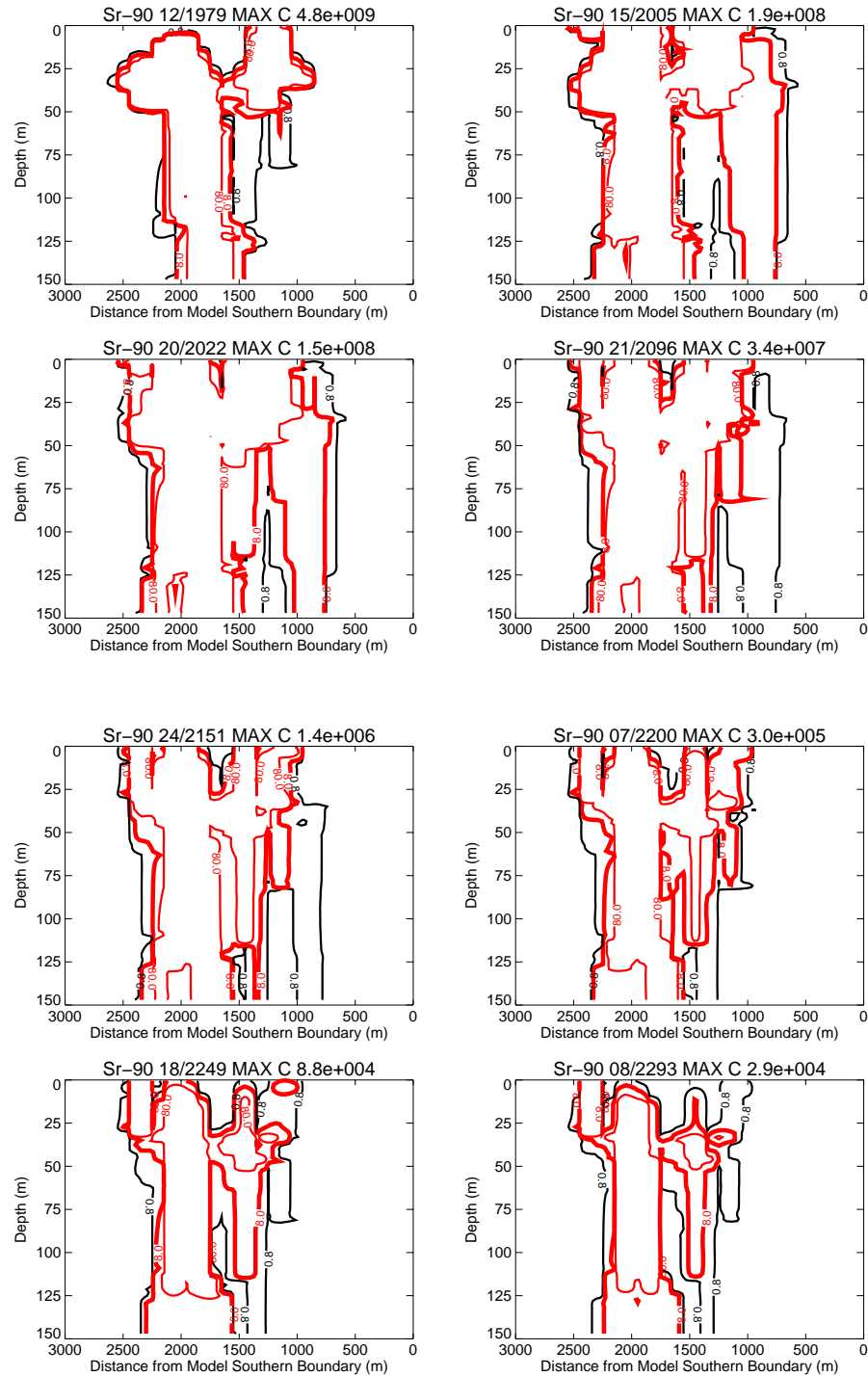


Figure A-5-3. Vadose zone concentrations (vertical contours) (pCi/L) reducing infiltration through the area surrounding the tank farm (MCL = thick red line, 10*MCL=thin red line, MCL/10 = black line).

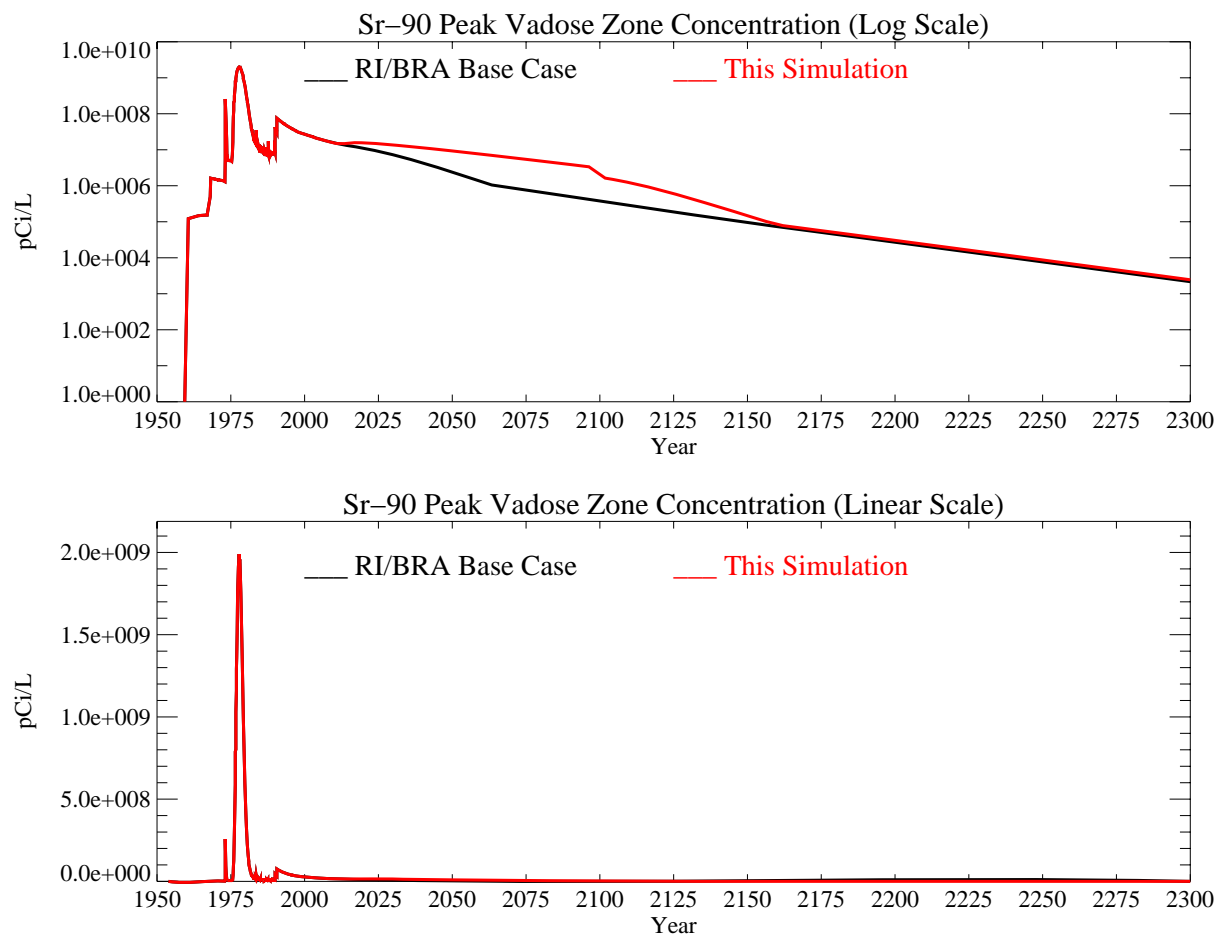


Figure A-5-4. Peak vadose zone concentrations (pCi/L) reducing infiltration through the area surrounding the tank farm (MCL = blue line, model predicted = black line [base case] and red line [this case]).

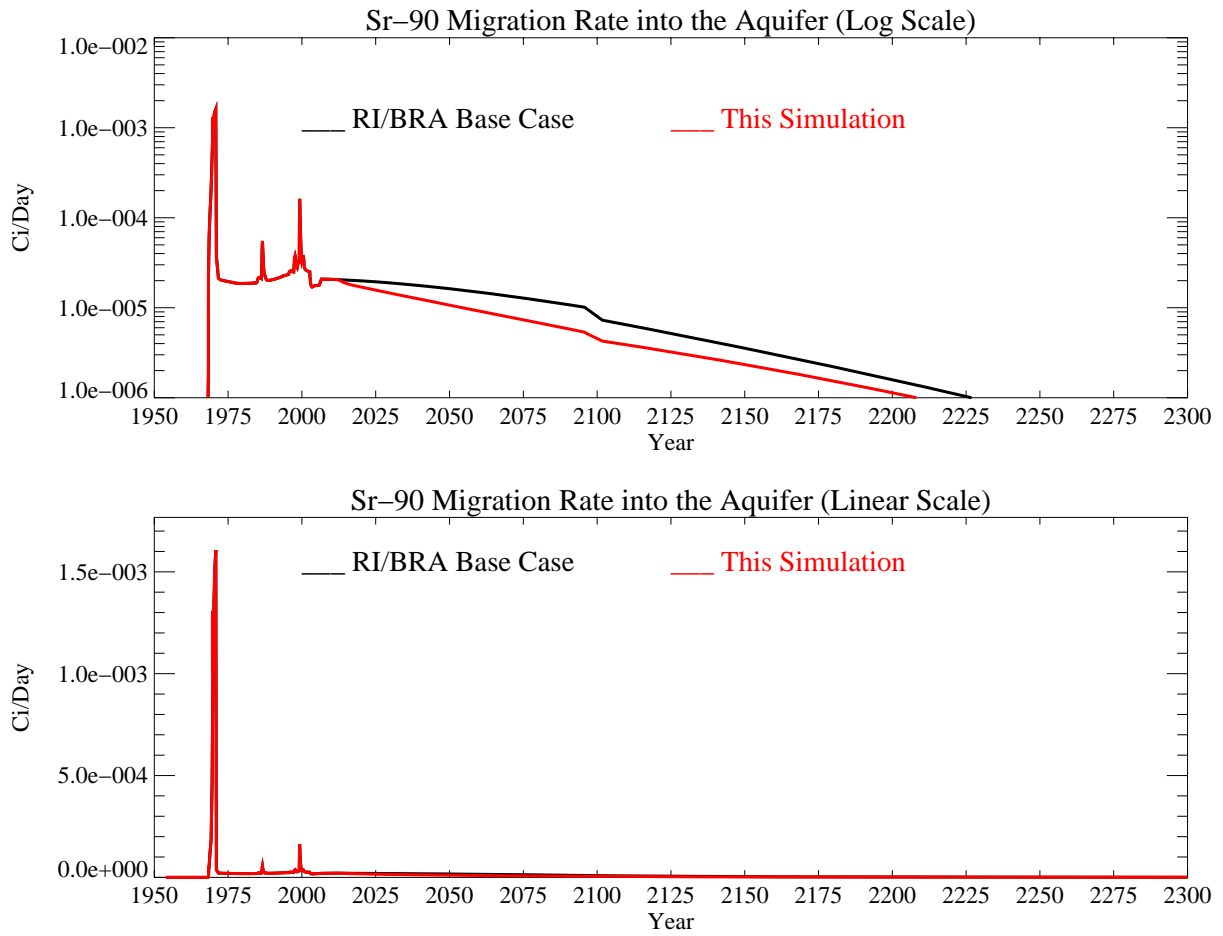


Figure A-5-5. Activity flux into the aquifer reducing infiltration through the area surrounding the tank farm (Ci/day).

A-5-2 Aquifer Sr-90 Simulation Results

Predicted Sr-90 concentrations in the aquifer through year 2096 on the course grid are shown in Figure A-5-6 and through the year 2151 on the fine grid in Figure A-5-7. These can be compared to the RI/BRA base case results shown in Figures J-8-18 and J-8-19 [DOE-NE-ID 2006]. Resultant peak aquifer concentrations for both simulations are shown in Figure A-5-8, with this simulation shown in red and the RI/BRA base case shown in black. There are three important performance measures illustrated in these figures. The first performance measure is the peak concentration in year 2095, the second is the time during which the MCL is exceeded, and the third is the areal extent contaminated above the MCL.

The predicted concentration in year 2095 is 7.9 pCi/L, which is significantly less than the 18.6 pCi/L predicted in the RI/BRA base case as shown in Figure A-5-8. This first performance measure suggests that reducing fluxes in central INTEC would be beneficial. Given the timing in response following this action, it is probable that the initial benefit is derived by reducing fluxes out of the deeper vadose zone. The long-term persistence is achieved by allowing more decay to occur in the upper perched water bodies.

The second performance measure is also significant as reflected by a reduction of 34 years during which the MCL is exceeded. In the RI/BRA base case, the MCL was exceeded through year 2129; after reducing infiltration through the area surrounding the tank farm, concentrations fall below 8 pCi/L in year 2095.

The area impacted above the MCL remains between the percolation ponds and south of the tank farm through year 2094 as shown in Figure A-5-7. However, with this relatively small decrease in flux, the area covered by Sr-90 above 0.8 pCi/L is only slightly smaller than predicted in the RI/BRA base case. The persistence of Sr-90 above 0.8 pCi/L is allowed by arrival from the vadose zone throughout INTEC as shown by the relatively unchanged shape of the 0.8 pCi/L isopleth.

These gains in all three performance measures were not achieved by immobilizing the Sr-90 in the alluvium as shown in Section A-4 but were derived because the highest vadose zone concentrations are predicted to be directly beneath the tank farm. By greatly reducing infiltration through the tank farm and through the area overlying the highest concentrations, a significant vertical driving force was removed. The roughly 25% of pore water originating from the Big Lost River and lateral influx from areas not directly beneath the tank farm still provide enough vertical transport that it takes until 2095 for concentrations to fall below the MCL. However, removing infiltration in the 10 acres surrounding the tank farm has increased the residence time in the vadose zone, allowing for decay to occur. It has also reduced the dispersive and advective transport.

This simulation suggests that actions being taken by OU 3-13 Group 4 to reduce infiltration might result in significant gains in aquifer concentrations. It also suggests that these reductions in fluxes should be targeted to areas above high perched water concentrations.

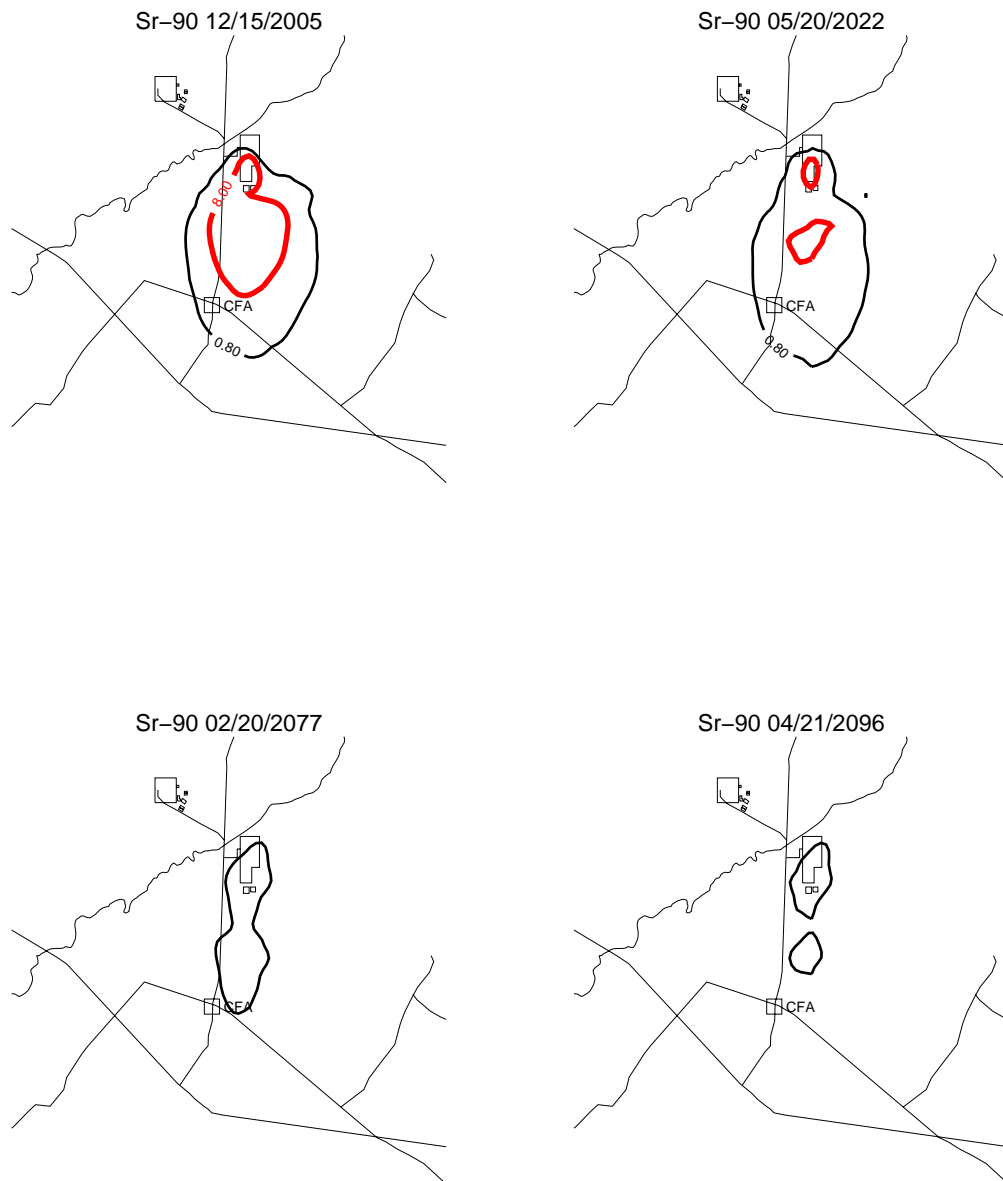


Figure A-5-6. Aquifer concentrations reducing infiltration through the 10 acres surrounding the tank farm (horizontal contours) (pCi/L) (MCL = thick red line, 10*MCL=thin red line, MCL/10 = black line).



Figure A-5-7. Aquifer concentrations reducing infiltration through the 10 acres surrounding the tank farm (horizontal contours) (pCi/L) (continued) (MCL = thick red line, 10*MCL=thin red line, MCL/10 = black line).

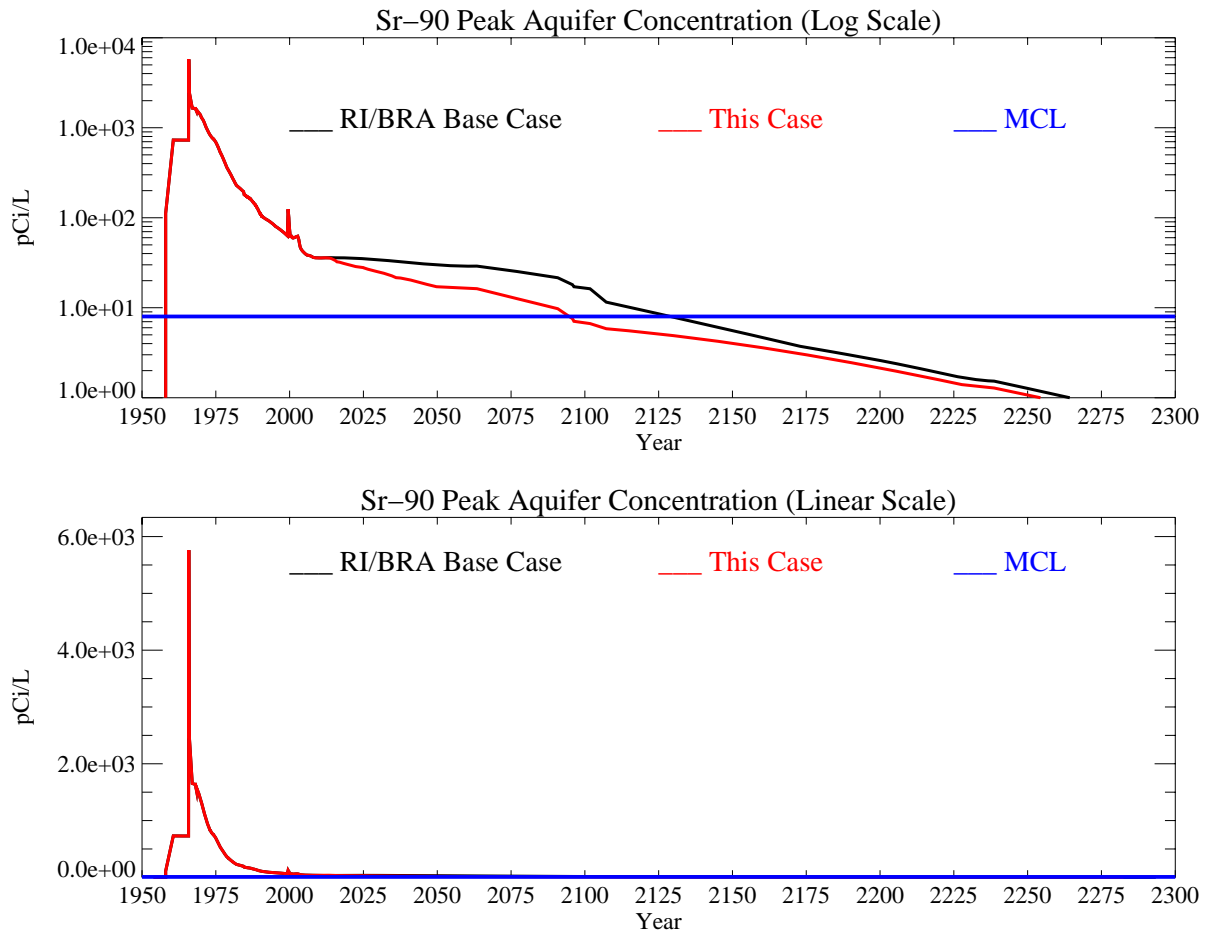


Figure A-5-8. Peak aquifer concentrations reducing infiltration through the 10 acres surrounding the tank farm (pCi/L) (MCL = blue line, model predicted = black line [base case] and red line [this case]).